Supporting Information for

Phase Transformation Fabrication of a Cu_2S Nanoplate as an Efficient Catalyst for Water Oxidation with Glycine

Li An,[†] Panpan Zhou,[†] Jie Yin,[†] He Liu,[†] Fengjuan Chen,[†] Hongyan Liu,[†] Yaping Du,[‡] and Pinxian Xi*[,†]

[†]Key Laboratory of Nonferrous Metal Chemistry and Resources Utilization of Gansu Province, State Key Laboratory of Applied Organic Chemistry and Colleague of Chemistry and Chemical Engineering, and The Research Center of Biomedical Nanotechnology, Lanzhou University, Lanzhou 730000, P. R. China

[‡]Frontier Institute of Chemistry, Frontier Institute of Science and Technology Jointly with College of Science, State Key Laboratory for Mechanical Behavior of Materials, Xi'an Jiaotong University, Xi'an 710049, P. R. China

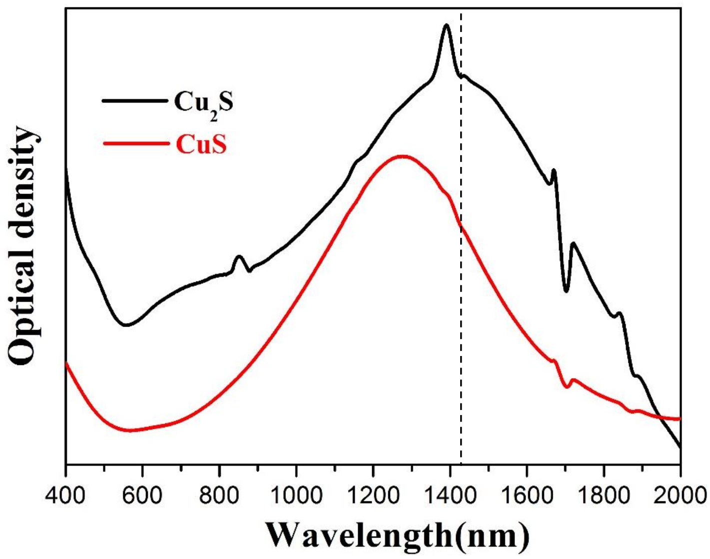

Figure S1. The near infrared absorption spectra of the CuS and Cu_2S NPs in chloroform.

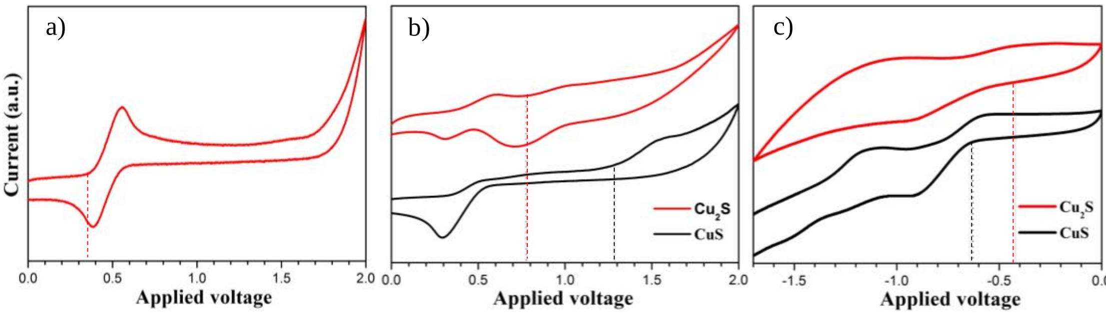

Figure S2. (a) The cyclic voltammograms (CV) of the oxidation potential of ferrocene as the internal standard to calibrate the measurements, and (b) oxide and (c) reduction CV of CuS (black line) and Cu_2S NPs (red line) .

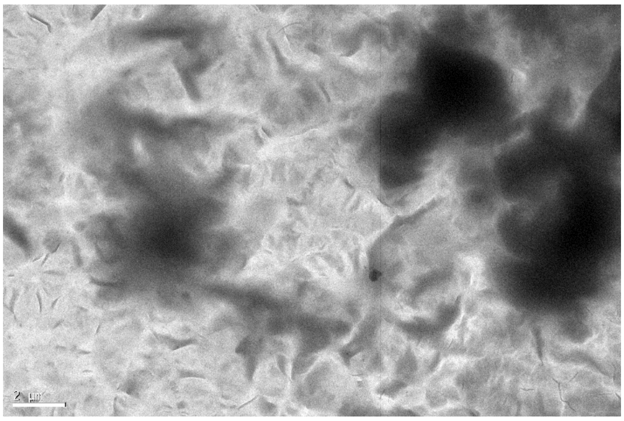

Figure S3. TEM of the CuS in ODE without OAm.

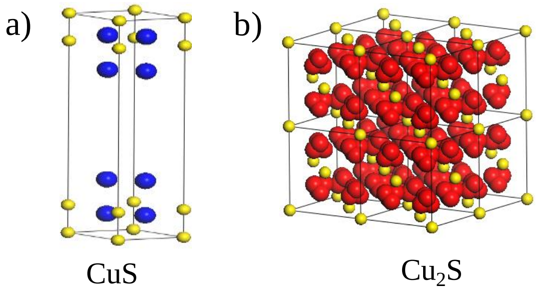

Figure S4. The crystal structure of (a) CuS NPs and (b) Cu_2S NPs.

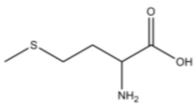

L-methionine

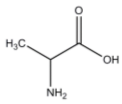

alanine

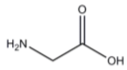

glycine

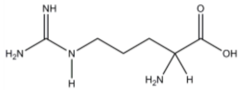

L-arginine

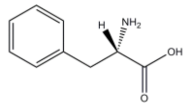

L-phenylalanine

Figure S5. The structure of the amino acids.

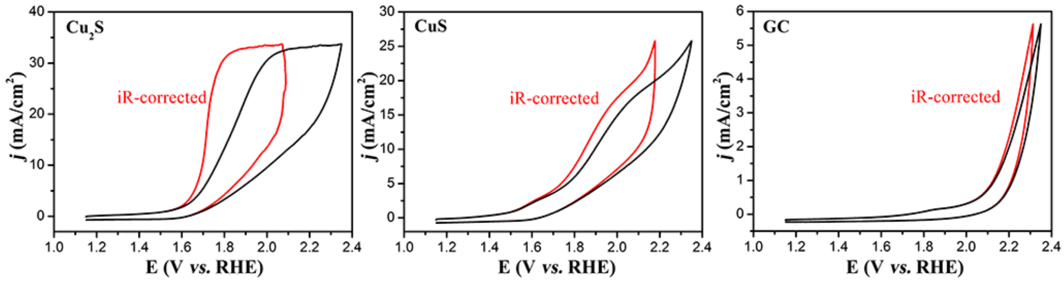

Figure S6. iR corrected CV of the Cu_2S, CuS and GC.

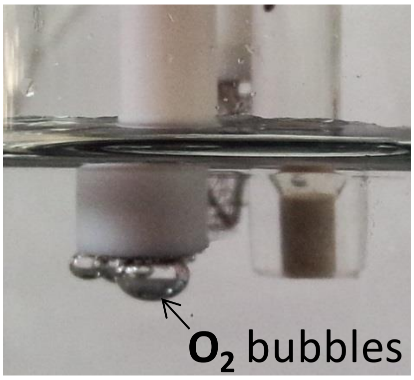

Figure S7. Optical photograph showing the generation of oxygen bubbles on Cu_2S NPs modified GCE.

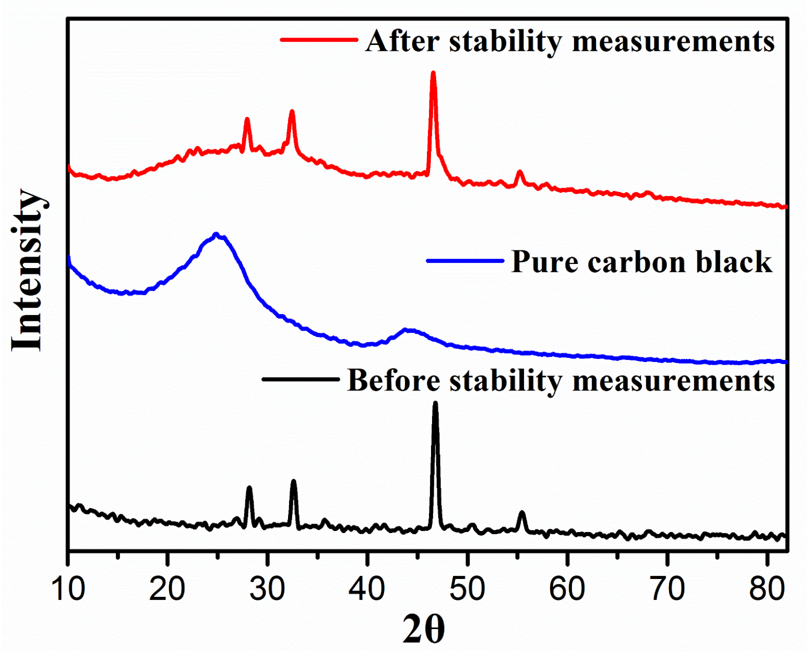

Figure S8. XRD pattern of the Cu_2S before and after the stability measurements.

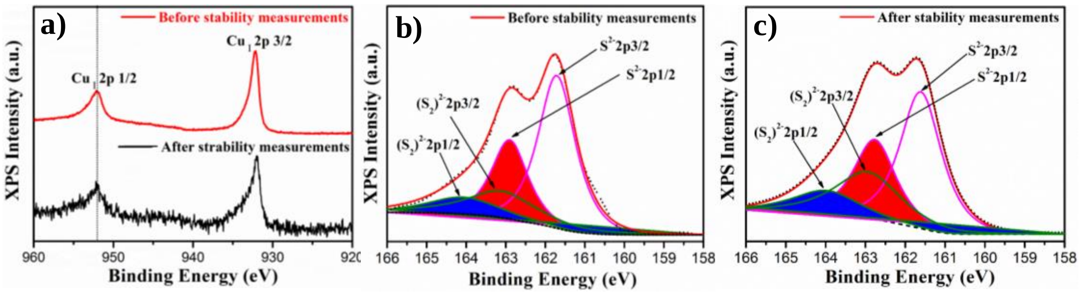

Figure S9. XPS spectra of a) Cu 2p, b) and c) S 2p of Cu_2S NPs before and after the stability measurements.

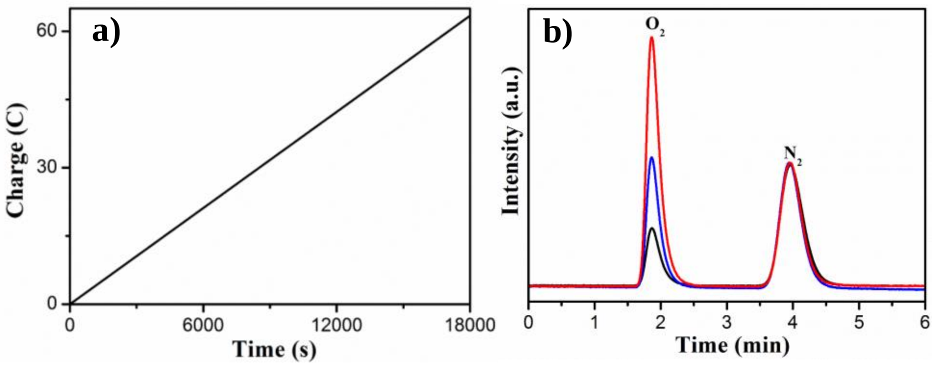

Figure S10. (a) Control potential electrolysis of a solution containing 6mM Gly. (b) Normalized gas chromatograms traces from a representative CPE experiment in the presence (red line) and absence (blue line) of 6 mM Gly. Black line shows the air background.

Table S1 Position of S $2p_{3/2}$ component for the sulfide and the disulfide doublets in the CuS and Cu_2S NPs.

Peak	BE(eV)	Area	FWHM(eV)	% GL (%)
CuS-$S^{2-}_{2p1/2}$	162.486	388.291	1.360	80
CuS-$S^{2-}_{2p3/2}$	161.286	657.122	1.360	80
Cu_2S-$S^{2-}_{2p1/2}$	162.898	890.085	0.990	80
Cu_2S-$S^{2-}_{2p3/2}$	161.640	1626.207	0.990	89
Cu_2S-$(S_2)^{2-}_{2p1/2}$	163.970	320.627	2.000	86
Cu_2S-$(S_2)^{2-}_{2p3/2}$	162.780	622.882	2.000	96

Table S2 The current and potential values of the Cu_2S with the addition of the small molecules.

Small molecules	**N, N dimethylformamide**	**N-acetylglycine**	**pyridine**	**acetate**
***j* [mA/cm^2]**	9.54	10.98	11.66	12.94
Potential [V *vs.* RHE]	2.02	2.04	2.04	2.00

Table S3 Comparison of OER performance of Cu_2S in Gly with other electrocatalysts in alkaline electrolytes.

Literature Citation	**Type of material**	**η at J = 10 mA cm^{-2} [mV]**
Iwakura, C.; Fukuda K.; Tamura, H. *Electrochim. Acta* **1976**, *21*, 501-508.	PtO_2	500
Morita, M.; Iwakura, C.; Tamura, H. *Electrochim Acta* **1979**, *24*, 357-362.	MnO_2	470
Iwakura, C.; Nishida M.; Tamura, H. *Nippon Kagaku Kaishi* **1982**, *7* , 1136-1140	$NiFe_2O_4$; $MgFe_2O_4$; $MnFe_2O_4$; $CoFe_2O_4$; $Li_{0.5}Fe_{2.5}O_4$	720; 780; 600; 450; 650
Raj, I. A.; Vasu, K. I. *International Journal of Hydrogen Energy* **1990**, *15*, 751-756.	Electrolytic manganese dioxide	>770
Izumiya, K.; Akiyama, E.; Habazaki, H.; Kumagai, N.; Kawashima, A.; Hashimoto, K. *Electrochimica Acta* **1998**, *43*, 3303-3312.	γ-MnO_2	790
El-Deab, M. S.; Awad, M. I.; Mohammad, A. M.; Ohsaka, T. *Electrochem. Communications* **2007**, *9*, 2082-2087.	Nanosized γ-MnOOH	1000
Kanan, M. W.; Nocera, D. G. *Science* **2008**, *321*, 1072-1076.	Co-oxide	570 (5 mA·cm -2)
Gorlin, Y.; Jaramillo, F. *J. Am. Chem. Soc.* **2010**, *132*, 13612-13614.	Nanostructured Mn (III) oxide	540
Wu, J.; Xue, Y. ; Yan, X.; Yan, W.; Cheng, Q.; Xie, Y. *Nano Res*. **2012**, *5*, 521-530.	Co_3O_4 /SWNTs hybrid	530
Wang, J.; Zhang, H.; Qin, Y.; Zhang, X. *Angew.Chem.Int. Ed.* **2013**, *52*, 5248-5253.	3D NF/PC/AN; Ni foam	534 (10.9 mA·cm -2) 564 (5 mA·cm -2)
Grewe, T.; Deng, X.; Weidenthaler, C.; Schüth,F.; Tüysüz, H. *Chem. Mater.* **2013**, *25*, 4926-4935.	Mesoporous Co_3O_4; Co_3O_4-$CuCo_2O_4$ Composite	528;498
Tüysüz, H. ; Hwang, Y. J.; Khan, S. B.; Asiri, A. M.; Yang, P. *Nano Res*. **2013**, *6*, 47-54.	Mesoporous Co_3O_4-100; Mesoporous Co_3O_4-35	636;525
Hardin, W. G.; Slanac, D. A.; Wang, X. Q.; Dai, S.; Johnston, K. P.; Stevenson, K. J. *J. Phys. Chem. Lett.* **2013**, *4*, 1254-1259.	$LaNiO_3$/NC	430
Liu, Q.; Jin, J.; Zhang, *J. ACS Appl. Mater. Interfaces* **2013**, *5*, 5002-5008.	$NiCo_2S_4$@N/S-rGO	470
Wang, D.; Chen, X.; Evans, D. G. ;Yang, W. *Nanoscale* **2013**, *5*, 5312-5315.	Co_3O_4/2.7Co_2MnO_4	540
Sa, Y. J.; Kwon, K.; Cheon, J. Y.; Kleitzc, F.; Joo, S. H. *J. Mater. Chem. A* **2013**, *1*, 9992-10001	Co3O4 NPs; CoO/CNT; Mesoporous Co3O4	449; 550; 525
Lee, D. U.; Kim B. J.; Chen, Z. *J. Mater. Chem. A* **2013**, *1*, 4754-4762.	$NiCo_2O_4$/G	440
Jin, C.; Lu, F.; Cao, X.; Yang, Z.; Yang, R.; *J. Mater. Chem. A* **2013**, *1*, 12170-12177.	$NiCo_2O_4$	490
Tian, J.; Liu,Q.; Asiri, A. M.; Alamry K. A.; Sun, X. ChemSusChem. **2014**, 7, 2125-2130.	Graphitic C_3N_4 Nanosheets /graphene Composites	539
Zhan, Y.; Xu, C.; Lu, M.; Liu, Z.; Lee. J. Y. *J. Mater. Chem. A* **2014**, *2*, 16217-16223.	MCF/N-rGO; MCF NPs; MCF/C; CFO/C; MFO/C	480; 610; 1.71;1.69;1.80

Wang, Y; Ding, W; Chen, S.; Nie, Y.; Xiong, K; Wei, Z. *Chem. Commun.* **2014**, *50*, 15529-15532	Cobalt carbonate hydroxide/C	509
Yu, X.; Sun, Z.; Yan,Z.; Xiang, B.; Liu, X.; Du, P. *J. Mater. Chem. A* **2014**, *2*, 20823–20831	$NiCo_2O_4$ nanowires	460
Cheng, N.; Liu. Q.; ian, J.; Xue, Y.; Asiri, A. M.; Jiang, H.; He, Y.; Sun, X.; *Chem. Commun*. **2015**, *51*, 1616-1619	Oxidized CC-8	477
This work	Cu_2S Nanoplate in Gly	428